JOURNAL OF MATERIALS SCIENCE **39** (2004) 1967– 1973

Investigation of the crack growth behavior of Inconel 718 by high temperature Moiré interferometry

XINGBO LIU*, B. KANG, W. CARPENTER, E. BARBERO
Department of Mechanical & Aerospace Engineering, West Virginia University, Morgantown, WV 26506-6106, USA
E-mail: Xingbo.Liu@mail.wvu.edu

The effect of environment on creep crack growth behaviors of many nickel-base superalloys is a well-documented and serious problem. Stress accelerated grain boundary oxidation (SAGBO) is accepted as the prior mechanism of the environment effect. In this paper, the crack growth behavior of Inconel 718 was investigated by high temperature moiré interferometry (HTMI), coupled with SEM/EDAX. Based on the results obtained from this research, the mechanism is proposed to be caused by the segregated Nb, which couples with the oxygen diffusing into the grain boundaries in front of the crack tip and forms an NbO layer on the grain boundaries, thereby causing the brittle elastic cracking behavior.

1. Introduction

Inconel 718 is a multi-component nickel-base superalloy with complicated structure i.e., γ'' and γ' strengthening phases precipitation in the grains and δ-phase precipitation at grain boundaries. Because of its properties, fabricability and cost effectiveness, Inconel 718 has gained more and more acceptance in various industries and has become the most widely used superalloy, accounting for 35% of all superalloy production in recent years [1]. To improve the alloy's performance and to better predict its service life, it is necessary to understand the processes of crack growth and sensitivity to environmental degradation behaviors of this alloy [2].

Two strong interactive mechanisms are responsible for much of the intergranular cracking, which is the weakest link in Inconel 718 as well as most other nickel-base superalloys at elevated temperatures. These are creep induced intergranular cracking and oxidation assisted crack growth. Further investigation reveals that creep and hold-time fatigue crack growth behaviors in nickel-base superalloys are environmentally sensitive. The crack growth rates in air can be as much as 1000 times faster than rates in an inert or vacuous environment [3–10]. Additionally, the incubation time for crack growth has been shown to be vastly greater in the inert environment as apposed to air. Those observations gave strong support to the conclusion that the creep crack growth of superalloys is principally due to the environmental degradation. It has been indicated that SAGBO plays the most important role in the environmental effect [11–14].

Moiré interferometry was developed in the 1980's and has been employed in a variety of areas in fracture mechanics, composite materials and interface mechanics [15, 16]. Moiré interferometry is capable of high resolution, full-field surface deformation measurements (up to 0.1 μm/fringe). For a typical moiré interferometry test, a grating is transferred onto the specimen surface to assume the same surface deformation as the specimen. Details of the optical principal of moiré interferometry can be found in reference [15]. In recent years, based on a chemical etching grating transfer procedure [17], we have developed a unique HTMI test method, which is capable of full-field displacement measurement under various environments (air, inert gas, oxygen, or vacuum) and at temperatures up to 1300°C [17–19]. In particular, we have demonstrated that the HTMI method can be applied to study crack growth behavior of metallic and intermetallic alloys for long testing duration under elevated temperatures [19].

Since creep and environmental effects happen at the same time during the creep crack propagation test in air, it is difficult to distinguish them from each other. Moreover, some new research results have shown that there is no increase in the crack growth rates of some alloys with increasing of hold-time, if the tests were done at higher temperature ($\geq$700°C). The purpose of this paper is to investigate the effects of creep and environment on creep crack growth behavior of Inconel 718 alloy at elevated temperatures. High temperature Moiré Interferometry (HTMI) was used to determine the full-field displacement of creep pre-cracked single edge notched specimens under sustained loading

*Author to whom all correspondence should be addressed.

TABLE I Chemical compositions of tested Inconel 718, wt%

Element	Ni	Fe	Cr	Ti	Nb	Mo	Al	C
Bar	Bal.	18.8	18.4	0.91	4.97	3.0	0.53	0.04

TABLE II Mechanical properties of the alloy at 650°C

Yield stress (MPa)	Young's modulus (MPa)	K_{th} (MPa$\sqrt{m}$)	K_{IC} (MPa$\sqrt{m}$)
1000	165,000	15	96.4

and various controlled oxygen-content environments. Based on the full-field crack tip moiré fringes, stress intensity factor, crack growth rates and crack tip plastic yield zone size and shape estimations were evaluated.

2. Experiments

2.1. Materials

The Inconel 718 alloy used for this research was provided by Special Metals Co., Huntington, WV. It was vacuum melted and the chemical compositions of the bar stock is given in Table I. The heat treatment given to the alloy is as following: 980°C/1 h/air cool + 718°C/8 h furnace cool to 621°C/18 h/air cool. Table II shows the alloy's mechanical properties at 650°C.

2.2. Specimens

Fig. 1 shows the Single-Edge-Notch (SEN) specimen geometry employed in this investigation. The specimens were cut perpendicular to the rolling direction so that the crack growth is parallel to the rolling direction. Table III gives the specific specimen dimensions for each of three test cases.

2.3. Crack growth test

Specimens were fatigue pre-cracked at room temperature and then creep crack growth tests were carried out at high temperature under constant load control. The atmosphere was controlled and the oxygen content was monitored by an Illinois Instruments 3000 Oxygen Analyzer.

TABLE III Specimen dimensions (mm)

Specimen	l	t	d	w	a	a/w
S1	130.5	1.95	10.0	25.25	10.0	0.396
S2	130.0	2.00	10.0	23.70	8.75	0.369
S3	140.0	1.85	10.0	24.35	13.7	0.563

2.4. High temperature Moiré interferometry set-up

Fig. 2 shows a schematic drawing of the optical setup. A specially-made loading apparatus was placed inside the vacuum chamber which allows a specified load to be applied to the test specimen. A quartz lamp heating set was placed near the specimen loading apparatus and a thermocouple is placed behind the specimen to monitor the test temperature. A residual gas analyzer was attached to the vacuum chamber to monitor the state of residual gases inside the chamber. A mechanical roughing pump, turbo pump, and ion pump are attached to the chamber so as to reach the desired vacuum level (as high as 10^{-8} torr is easily achievable). Four (one inch diameter) collimated laser wavefronts were directed onto the test specimen (two shown in Fig. 2) and the resulting

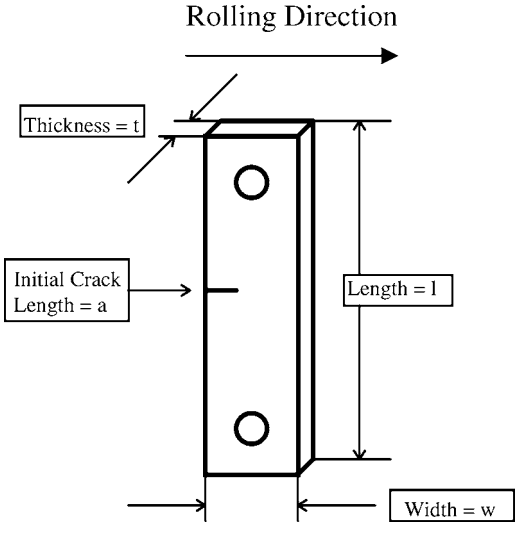

Figure 1 Geometry of the single-etch-notch specimen.

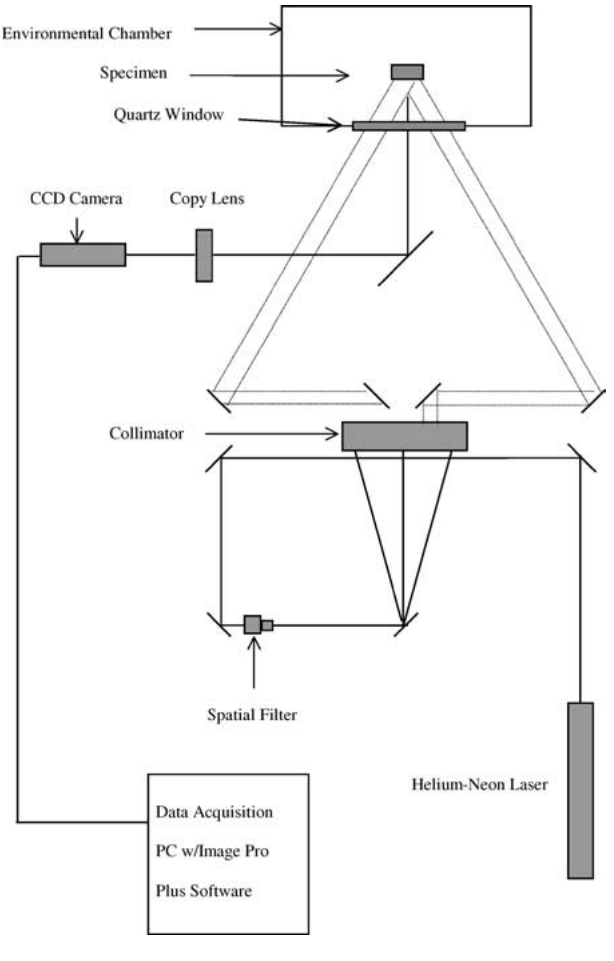

Figure 2 Schematic of Moiré interferometry set-up.

moiré fringes were then related to the specimen surface deformation [15]. The moiré images were captured using a pc-based image acquisition system.

Typically, a testing procedure using Moiré Interferometry, includes the following:

- Adjustment of the optical alignment to obtain the initial null field at room temperature.
- Gradual increase of temperature in small steps of 30–50°C, up to the testing temperature, ensuring that the specimen is subjected to a uniform thermal load.
- Readjustment of the fringe pattern to a null-field at the final testing temperature.
- Gradual load increase and recording of the corresponding full-field crack-tip moiré fringes.

2.5. Fractography and microstructure analysis

The fractography and microstructure analysis were mainly performed with a Hitachi S-570LB scanning electronic microscope (SEM) with Kevex EDAX system for chemical analysis. Some additional work was carried out using Jeol 6400SEM with PG&T EDAX.

3. Results and discussion

3.1. Crack propagation and environmental effect

The test sequence and crack growth behaviors of 3 specimens were listed in Table IV. Specimen 1 was loaded in pure argon for 6 days and there was still no observed crack growth. After one day's loading in pure argon with no observed crack growth for Specimen 2, crack growth was found at 52 min after introducing pure oxygen flow through a retort. The comparison between 1 and 2 clearly show that the environmental effect is the prime reason of the crack growth for Inconel 718 under sustained loading.

3.2. Plastic zone development

Moiré fringe patterns of the crack tip region were recorded periodically throughout each testing sequence. A sample of the results for Specimen 3 is presented in Fig. 3. The Moiré patterns were analyzed and a plastic yield zone and its shape were constructed for this test. Previous research has shown that analysis of Moiré fringes to replicate the plastic yield zone size [16, 20] and shape are indeed a close approximation to the LEFM prediction [21]. Plastic yield zone size and shape for selected times throughout the experiment are presented in Fig. 4a–c. Moiré fringes can be divided into v- and u-fields. The v- and u-fields represent displacement fields perpendicular and parallel to the crack direction, respectively. The Moiré fringes are formed when load is applied to the specimen. They represent constant displacement contours, i.e., any point within a fringe has the same displacement. In this research, the displacement gradient between any two adjacent moiré fringes was 0.8 μm. Note that, for all the Moiré fringes shown in this paper, the zero v-field is a horizontal line starting from the crack tip toward the right. During this investigation, only v-field Moiré fringes were recorded, therefore only ε_y was calculated. To produce the plastic yield zone estimation, ε_y was compared to the yield strain to determine the elastic-plastic boundary. Since ε_x was not taken into account, at low θ values (where θ is measured from the axis of the crack tip) these estimations likely underestimate the magnitude of the plastic yield zone radius. However, the results still show the plastic zone development during the test. As the load is constant, theoretically the plastic yield zone must be the same, but the comparison between Fig. 4a and b shows that the plastic yield zone becomes larger after 6 days of testing. In addition, the shape of the zone changed. This phenomenon can be attributed to the creep development during the test. Creep development is not homogenous because of the stress concentration in front of the crack tip; therefore the shape of plastic yield zone is changed after 6 days of testing. Fig. 4c shows that the plastic yield zone size increases as the increase of stress intensity factor.

TABLE IV Crack growth behavior of Inconel 718

Specimen	1	2	3
Step 1			
Temperature	650°C	650°C	650°C
Time	6 days	1 day	10 days
K	48 MPa$\sqrt{}$m	42 MPa$\sqrt{}$m	42 MPa$\sqrt{}$m
Environment	Argon	Argon	Argon
Behavior	No growth	No growth	No growth
Step 2			
Temperature	Stop	650° C	650°C
Time		120 min	366 min
K		42 MPa$\sqrt{}$m	42 MPa$\sqrt{}$m
Environment		Oxygen $P = 10$ tor	Oxygen $P = 10$ tor
Behavior		Growth after 52 min	Growth after 281 min

3.3. Creep effects

Since creep and environmental effect happen at the same time during the creep crack propagation test in air, it is difficult to distinguish them between each other. However, if the test is carried out in vacuum or inert gas, creep effect can be revealed independently since there is no environmental effect. Fig. 5 shows the crack growth behaviors of Specimens 2 and 3. The beneficial effect of creep is revealed by comparing the test results of Specimen 2 with that of Specimen 3. Both specimens were exposed to Argon for certain time and then oxygen was introduced, after a certain incubation time, the crack started to grow. However, compared with Specimen 2, Specimen 3 has longer incubation time (281 min for Specimen 3 vs. 52 min for Specimen 2) and lower crack growth rates, which is shown in Fig. 5. The initial loading condition is the same for both specimens, stress intensity factor is equal to 42 MPa$\sqrt{}$m. The difference between them is that Specimen 3 was exposed in argon for 9 days more than Specimen 2, which means there is more creep development for Specimen 3 than Specimen 2.

During the creep crack growth test, the creep behavior of the specimen is not homogeneous because

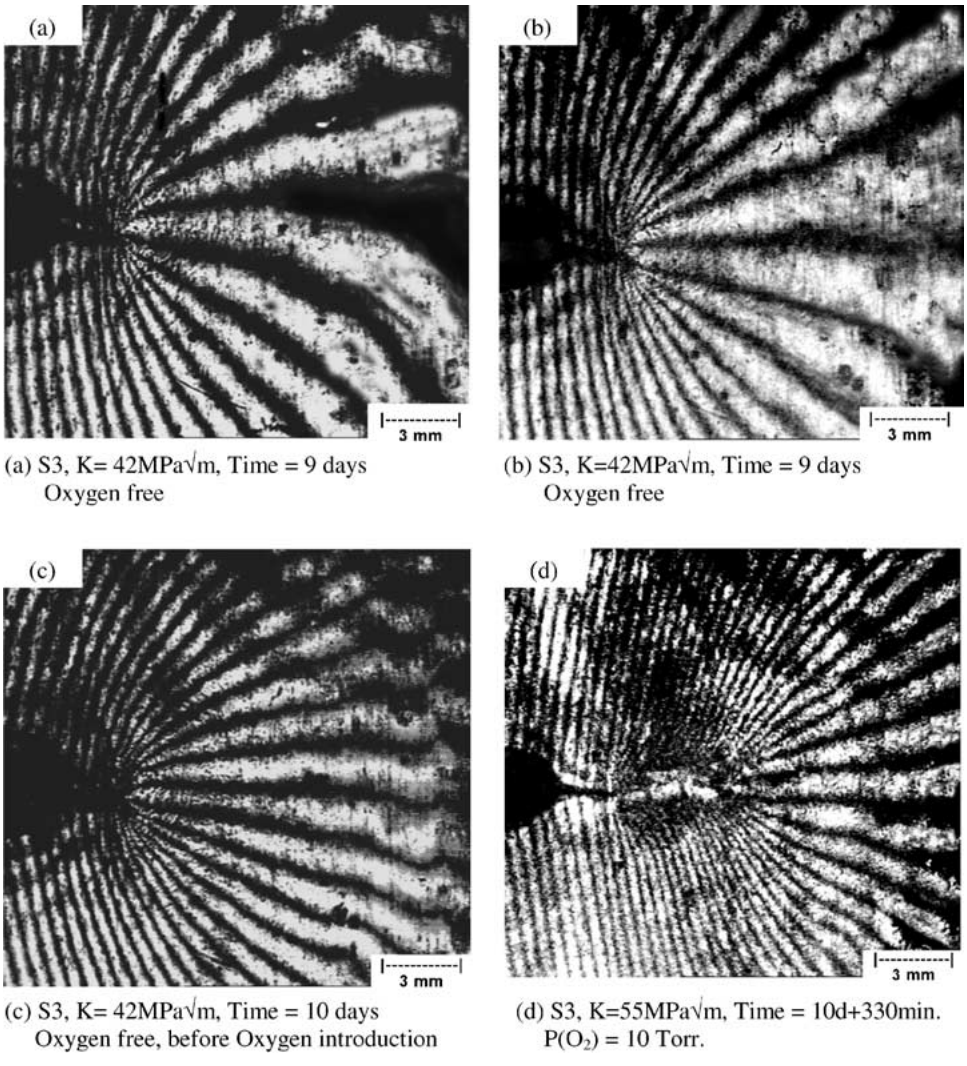

Figure 3 Moiré fringe patterns of Specimen 3 during the crack growth test.

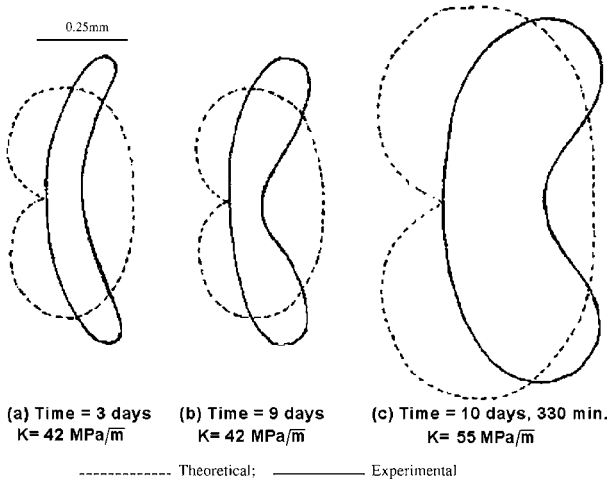

Figure 4 Plastic yield zone development during the test, Specimen 3.

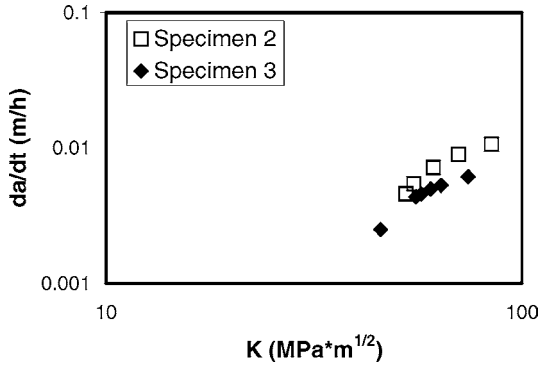

Figure 5 Creep crack growth of Inconel 718 SENT Specimens 2 and 3. $T = 650°C$, delayed oxygen atmosphere.

of stress concentration in front of the crack tip. Fig. 6 sketches creep development in front of the crack tip during the crack growth test. At the beginning, there is only a primary creep zone in front of the crack tip. As creep develops, steady state creep zone appears, which is surrounded by the primary creep zone. During the last stage of the test, there is a tertiary creep zone developed, which is surrounded by steady state and primary creep zones and there are large amount of creep cavities inside this zone.

Riedel etc. [22, 23] analyzed the creep behavior in front of the crack tip. If a load is applied and then held constant, a creep zone gradually develops in the plastic zone. They proposed that the stresses well within the creep zone could be described by:

$$\sigma_{ij} = \left(\frac{C(t)}{AI_n r}\right)^{\frac{1}{n+1}} \hat{\sigma}_{ij}(n, \theta) \qquad (1)$$

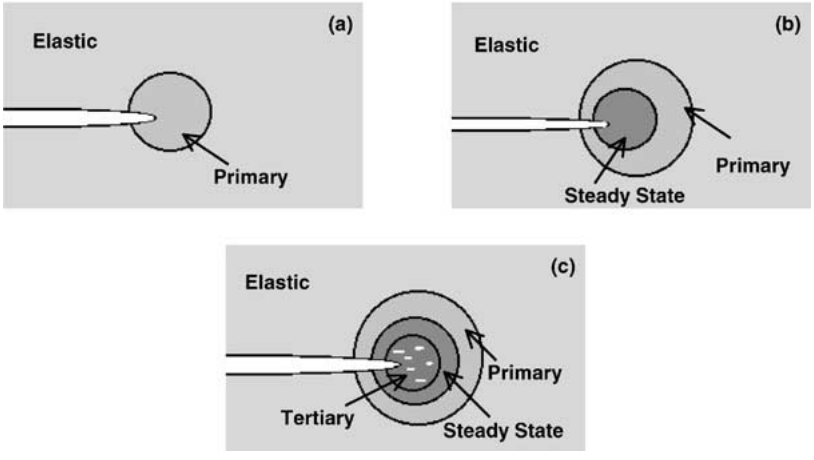

Figure 6 Sketch of creep development in front of the crack tip during crack growth test.

where n is the exponent in the creep equation, A, I_n are numerical constants, $\hat{\sigma}_{ij}(n, \theta)$ is a variable which is a function of n and θ, r is the distance from the crack tip. $C(t)$ is a parameter that characterizes the amplitude of the local stress singularity in the creep zone.

$$C(t) = \frac{K_I^2(1-\upsilon)^2}{(n+1)Et} \tag{2}$$

where K_I is mode I stress intensity factor, υ is the Poisson ration, E is the Young's modulus ant t is hold-time. $C(t)$ varies with time and is equal to C^* in the limit of long time behavior [24]. If the remote load is fixed, the stresses in the creep zone relax with time, as creep strain accumulates in the crack tip region. The "effective" stress is lowered by stress relaxation during hold time, which shows that creep plays a beneficial role on crack growth by stress relaxation.

3.4. Mechanism of SAGBO

Based on the comparative results of a large amount of crack growth tests in vacuum and in air or other aggressive environments [3–9], environmental effects have been shown to play a major role in time-dependent creep or fatigue crack propagation for most superalloys. It is important to note that according to many investigations [25, 24], environment did not produce such significant attack in unstressed materials. Therefore, SAGBO has been considered to be responsible for time-dependency of creep and fatigue crack propagation. It is assumed that the materials' resistance to crack growth is reduced as oxygen in front of the crack tip diffuses into the grain boundary and then crack can pass through the damage zone. However, in spit of numerous publications on this topic, the detailed mechanism of SAGBO still remains unclear. In this investigation, extensive post-test microstructural analysis of the crack region for Specimens 2 and 3 was performed to determine the actual mechanism of the SAGBO embrittlement phenomenon of Inconel 718.

Fig. 7 shows the overall crack growth path of Specimen 3. Based on this sequence of pictures, it was ascertained that the crack growth was indeed intergranular with many secondary-cracks branching out from the main crack. It is also indicated that there is a white film network along the grain boundaries of the crack path. Upon further enlargement of the crack tip area using SEM, areas of grain boundary particle formation were more readily detected. Fig. 8 shows the last propagation of the crack for Specimen 3. The particles on the fractured grain boundaries can be found in this micrograph. EDAX mapping was conducted on the particle

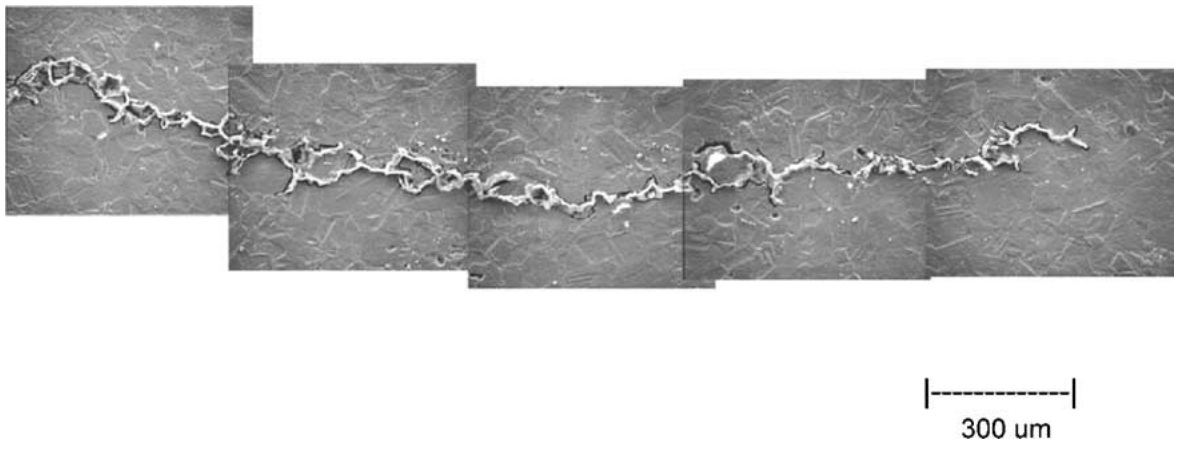

Figure 7 SAGBO-induced creep crack growth sequence, Specimen 3.

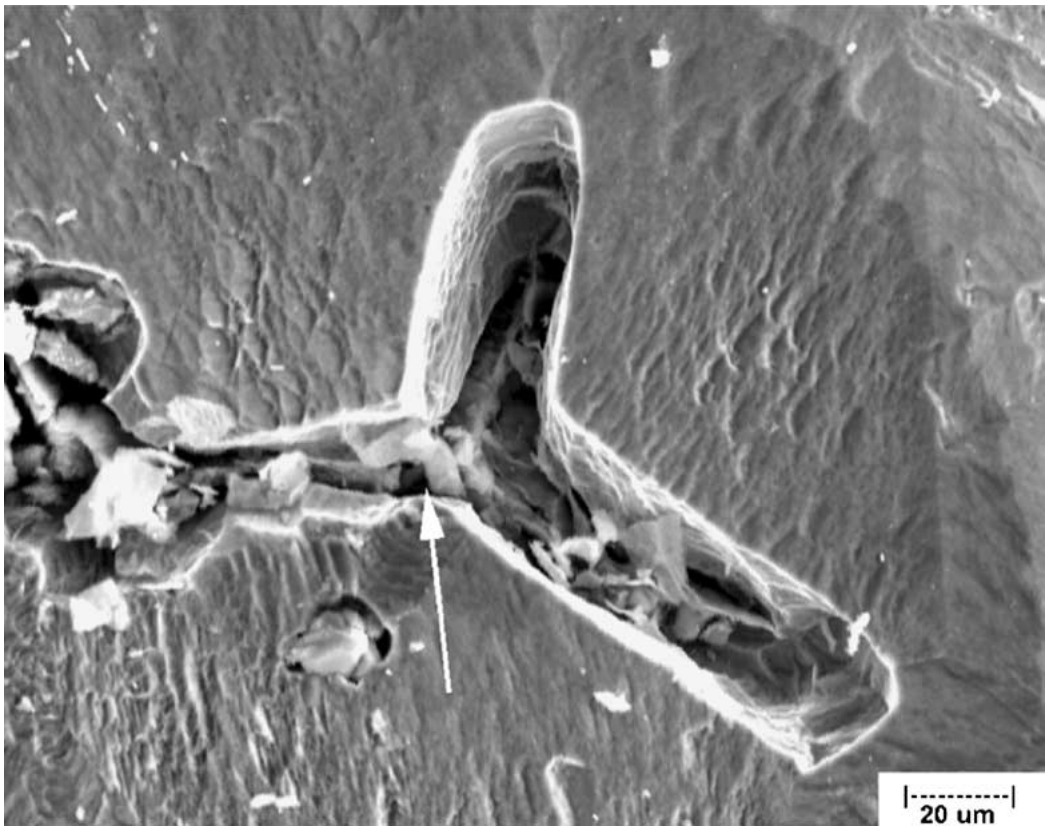

Figure 8 Enlargement of crack tip region, Specimen 3. (Arrow indicates particle studied)

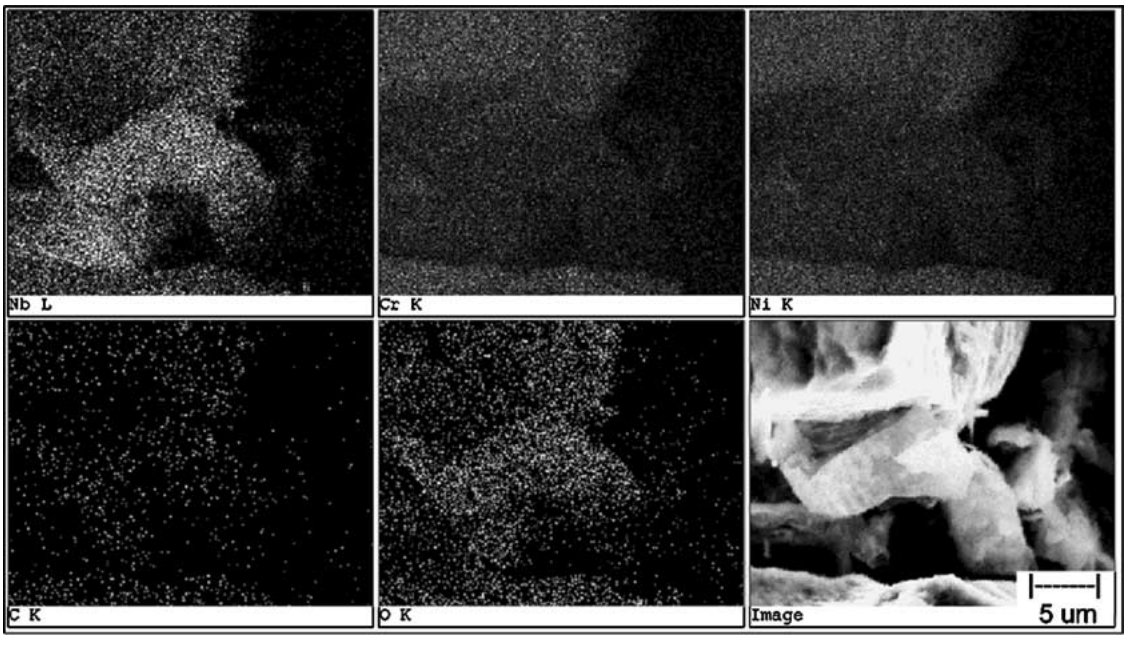

Figure 9 EDAX map of the particle indicated in Fig. 8, Specimen 3.

in Fig. 8 and the result is shown as Fig. 9. It is clear that there are niobium oxide particles in the expanded grain boundaries on the fracture path.

Fig. 10 shows the EDAX Spectra of grain boundary and matrix of Inconel 718. It is clear that comparing with the matrix, the contents of niobium and titanium at the grain boundary are much higher. In addition, previous Auger results confirm that niobium, titanium along with chromium, strongly segregate to the grain boundaries of Inconel 718 [26, 27]. It was also demonstrated by Auger and SIMS results that oxygen can diffuse to regions well ahead of the crack tip [28]. Therefore, based on the experimental results in this investigation, the mechanism of SAGBO in Inconel 718 is concluded to be caused by the diffusion of oxygen under high stress levels in front of the crack tip coupled with segregation of niobium at the grain boundaries and formation of brittle niobium oxide layer along the grain boundaries. The fracture of brittle niobium oxide layer under the concentrated stress in front of the crack tip leads to the

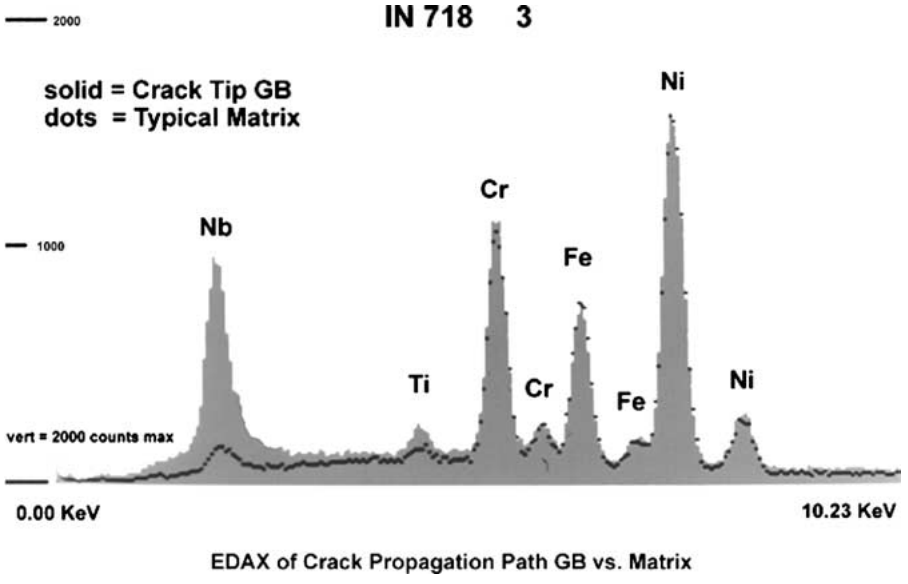

Figure 10 EDAX Spectra of grain boundary and matrix of Inconel 718, Specimen 3.

crack growth and causing the brittle elastic cracking behavior.

4. Conclusions

The crack growth behaviors of Inconel 718 were investigated by High Temperature Moiré Interferometry along with SEM/EDAX analysis. Several conclusions were drawn based on the experimental results.

1. The crack growth behavior of the alloy under sustained loading is caused by environmental effect instead of creep effect. Stress Assisted Grain Boundary Oxidation (SAGBO) is found as the mechanism of the environmental effect.

2. Niobium tends to segregate towards the grain boundaries of the alloy. The segregated Nb couples with the oxygen diffusing into the grain boundaries in front of the crack tip and form NbO layer, which is brittle and easy to break under the concentrated stress in front of the crack tip. Therefore, it provides fast growth pass of the crack.

3. Long-term aging coupled with stress concentration around the crack tip leads to creep development and stress relaxation, which are beneficial to the alloy's resistance against the crack growth.

References

1. E. A. LORIA, *J. Metals* **7** (1995) 32.
2. M. GAO, D. DWYER and R. WEI, in "Superalloys 718, 625, 706 & Various Derivatives," edited by E. A. Loria (TMS, 1997) p. 581.
3. S. LYNCH, *Acta Met.* **36** (1988) 2639.
4. M. STROOSNIJDER, V. GUTTMANN and J. H. W. DE WIT, *Met. Mat. Trans.* A **26A** (1995) 2103.
5. MCEVILY and J. L. VELAZQUEZ, *Met. Trans.* A **23A** (1992) 2211.
6. H. SMITH and D. MICHEL, *ibid.* **17A** (1986) 370.
7. VASATIS and R. PELLOUX, *ibid.* **16A** (1985) 1515.
8. L. KORUSIEWICZ, J. DONG and M. KUMOSA, *Scripta Met. et Mater.* **29** (1993) 573.
9. E. FLEURY and L. REMY, *Mater. Sci. Eng.* **A167** (1993) 23.
10. P. N. CHAKU and C. J. MCMAHON JR., *Met. Trans.* A **5** (1974) 441.
11. C. J. MCMAHON and L. F. COFFIN JR., *ibid.* **1** (1970) 3443.
12. D. A. WOODFORD, *ibid.* A **12A** (1981) 299.
13. P. SHAHINIAN and K. SADANANDA, Superalloy 1984, edited by M. Cell, C. S. Kortouich, R. H. Brickaell, W. B. Kent, and J. Radavich (TMS, 1984) p. 741.
14. I. VASATIS and R. PELLOUX, *Met. Trans.* A **16A** (1985) 1515.
15. D. POST, "Handbook for Experimental Stress Analysis," Chapter 7 Moiré Interferometry, edited by A. S. Kobayashi (Prentice Hall, 1987) p. 314.
16. D. POST, B. HAN and P. IFJU, "High Sensitivity Moiré: Experimental Analysis for Mechanics and Materials" (Springer Verlag, Berlin, 1997).
17. B. S.-J. KANG, G. Z. ZHANG, M. G. JENKINS, M. FERBER and P. IFJU, ATEM '93 Conference on Advanced Technology in Experimental Mechanics (1993) p. 207.
18. B. S.-J. KANG, G. ZHANG, P. LIU and M. ELLATHUR, 1995 ASME Winter Conference, San Francisco, CA, November, 20–24 (1995).
19. W. CARPENTER, B. S.-J. KANG and K. M. CHANG, "Superalloys 718, 625, 706 and Derivatives" (TMS, 1997) p. 679.
20. B. KANG, X. LIU *et al.*, *Mater. Sci. Engng.* A **A347** (2003) 205.
21. T. ANDERSON, "Fracture Mechanics" (CRC Press, Boca Raton, 1994) p. 78.
22. *Idem.*, "Fracture Mechanics" (CRC Press, Boca Raton, 1994) p. 230.
23. H. RIEDEL and J. R. RICE, *ASTM STP* **700** (1980) 112.
24. J. LARSON and S. FLOREEN, *Met. Trans.* A **8A** (1977) 51.
25. S. FLOREEN and R. KANE, *ibid.* **10A** (1979) 1745.
26. J. DONG, X. XIE and R. THOMPSON, *ibid.* **31A** (2000) 2135.
27. J. DONG, X. LIU, *et al.*, *Acta Metall. Sinica* (*English Letters*) **10** (1997) 510.
28. T. S. SUDARSHAN and M. R. LOUTHAN JR., *Int. Mat. Rev.* **32** (1987) 121.

Received 5 June
and accepted 28 October 2003